Metal to insulator transition in the *n*-type hollandite vanadate $Pb_{1.6}V_8O_{16}$

A. Maignan,[1] O. I. Lebedev,[1] G. Van Tendeloo,[2] C. Martin,[1] and S. Hébert[1,*]
[1]*Laboratoire CRISMAT, UMR 6508 CNRS/ENSICAEN, 6 bld. du Maréchal Juin, F-14050 CAEN Cedex 4, France*
[2]*EMAT, University of Antwerp, Groenenborgerlaan 171, B-2020 Antwerpen, Belgium*
(Received 16 March 2010; revised manuscript received 25 June 2010; published 27 July 2010)

The transport and magnetic measurements of polycrystalline $Pb_{1.6}V_8O_{16}$ hollandite reveal a concomitant metal to insulator and antiferromagnetic transition at $T_{MI} \approx 140$ K. A clear localization is found below T_{MI}, evidenced by a rapid increase in the absolute value of the negative Seebeck coefficient. The structural study by x-ray and transmission electron microscopy confirms the hollandite structure and shows that no structural transition occurs at T_{MI}, ruling out a possible charge orbital ordering. The negative Seebeck coefficient observed from 50 K up to 900 K, with values reaching $S=-38$ μV K^{-1} at 900 K, is explained by the electron doping of $\sim 1.4e^-$ in the V empty t_{2g} orbitals responsible for the bad metal resistivity ($\rho_{900\ K} \sim 2$ mΩ cm). As this S value is close to that obtained by considering only the spin and orbital degeneracies, it is expected that $|S|$ for such vanadates will not be sensitive at high temperature to the t_{2g} band filling.

DOI: 10.1103/PhysRevB.82.035122 PACS number(s): 72.80.Ga, 71.30.+h, 72.15.Jf

I. INTRODUCTION

These last years, the transition-metal oxides (TMOs) exhibiting mixed valency have attracted much attention for the richness of their physical properties (superconductivity, magnetoresistance, thermoelectric properties, …). Regarding these properties, one can quote cuprates, manganites, or cobaltites all containing 3*d* cations, for which the strong electronic correlations are responsible for spin/orbital/lattice coupling phenomena.[1] Furthermore, the low structural dimensionality in TMO is often necessary to generate such properties like the two-dimensional (2D) character of the CuO_2 planes in the high T_c's or like the one-dimensional (1D) reduced dimensionality of the $S=1/2$ spin ladders.[2]

The need for new thermoelectric (TE) materials, stable in air, operating well beyond room temperature (RT) becomes a very active research field in materials science as the recovery of waste heat into electricity by using TE generators is a very interesting technology to lower the consumption of cars and trucks. This explains why thermoelectric TMOs are deeply studied.[3] At present, TE TMO *p*-type cobaltites have been found but their performing *n*-type counterparts are still missing. To explain the *p*-type cobaltites TE properties, the concept of spin-orbital engineering has been proposed by Koshibae[4] following previous study of Marsh and Parris:[5] for high enough T, the Seebeck (S) value saturation comes from an extra term in the Heikes formula $\Delta S_d=(k_B/e)\ln(\Gamma_{orb}\Gamma_{spin})$, where Γ_{orb} Γ_{spin} are for the orbital and spin degeneracies of the cations involved in the mixed valency. In contrast, the physics of the *n* type is rather different and at first glance a more conventional metal-like behavior $S\alpha T$ is measured (for doped $CaMnO_3$, $SrTiO_3$, ZnO, and In_2O_3) but with a large dS/dT slope, leading to rather high $|S|$ values for $T \gg 300$ K.[6] In principle, for TE materials, the low dimensionality allows to enhance the Seebeck coefficient since according to the relation $S\alpha[\partial \ln d(E)/\partial E]_{E=E_F}$, the sharpness of the density of states $d(E)$ at E_F increases with decreasing the dimensionality. In addition, the low structural dimensionality in a 2D or 1D crystalline framework limits the phonon propagation which makes decreasing the thermal conductivity κ. Both trends are supposed to contribute to the figure of merit Z enhancement as $Z=S^2\sigma/\kappa$ (σ and κ are the electrical and thermal conductivity, respectively). Looking for *n*-type oxides having 3*d* cations with a mixed valency and a low structural dimensionality, it appears that compounds with hollanditelike structures[7] might be of interest. In that structure, the double rutile ribbons of edge-shared TMO_6 octahedra can be viewed as TM-TM triangular ladders. Similar ribbons are also encountered in the $CaFe_2O_4$ structure as for instance CaV_2O_4.[8] In the hollandite structure, the network resulting from the corner sharing of these ribbons leads to a TM_8O_{16} hollandite framework delimiting "square" section channels occupied by counterions (K^+,Ba^{2+},Bi^{3+},…) (see insets of Fig. 1). Although metal-insulator transitions (MITs) have already been reported for vanadate hollandites $Bi_xV_8O_{16}$ (Ref. 9) and $K_2V_8O_{16}$,[10] not much is known about the T-dependent properties of $Pb_xV_8O_{16}$, a compound discovered by Mentre and Abraham.[11] In the following we re-

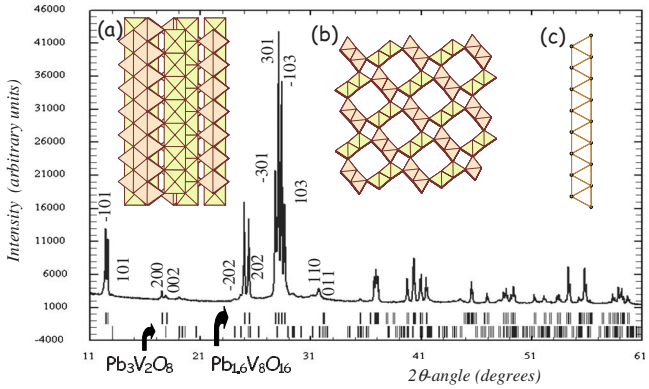

FIG. 1. (Color online) Small-angle part of the RT x-ray diffraction pattern in which the first indexations corresponding to $Pb_{1.6}V_8O_{16}$ are given ($I12/m1$ with $a=10.125$ Å, $b=2.902$ Å, and $c=9.880$ Å, $\beta=90.928°$). Drawings of the structure are given in the insets, to show the two kinds of VO_6 double chains running along the *b* axis in (a), to highlight the tunnels delimited by four couples of VO_6 units, using a projection in the (a,c) plane in (b) and schematized triangular V ladder along *b* in (c).

port on the *T*-dependent structural, electronic, and magnetic properties of polycrystalline $Pb_{1.6}V_8O_{16}$ hollandite. This *n*-type compound exhibits a metal to insulator transition at 140 K. By transmission electron microscopy, at 100 K, no extra peaks related to V^{3+}/V^{4+} charge ordering could be detected. The Seebeck coefficient measured up to 1000 K, shows that $|S|$ increases with *T* over a large range from ~180 to 900 K reaching $S=-38$ μV K^{-1} at 900 K. This MIT can also be compared to the ones investigated in other vanadium oxides with different structures such as $La_{1-x}Sr_xVO_3$ perovskites with corner-shared octahedra, V_2O_{3-y} with corundum structure, or VO_2 with rutile structure (for a review see Ref. 12).

II. EXPERIMENTAL

The ceramics were obtained by solid-state reaction in evacuated silica tubes. 1 g of $Pb_{1.6}V_8O_{16}$ powder was prepared by mixing in a glove box the precursors, PbO, V_2O_3, and V_2O_5 in the stoichiometric ratio. The powder was then pressed in bars ($2\times2\times10$ mm^3) inserted in alumina crucibles, which were set in silica tubes pumped under primary vacuum prior to sealing. The closed ampoules were heated at 900 °C for 12 h. The structure of the reacted black products was first studied by refinements of the RT x-ray powder-diffraction data (Cu $K\alpha$ radiations and a $10°-110°$ 2θ range) using FULLPROF.[13] The structure and composition were also determined by using a JEOL-4000EX transmission electron microscope (TEM) for imaging at high resolution and a Philips CM20 to perform electron diffraction (ED) and low temperatures (LTs). TEM measurements were made on a crushed sample, dissolved in methanol and deposited on a holey carbon grid. The magnetic properties were measured using a superconducting quantum interference device magnetometer (zero-field-cooling warming, field-cooling warming, and cooling) within a magnetic field of 0.3 T. The four-probe method and a steady-state technique were used to measure the electrical resistivity ρ and the Seebeck coefficient *S*, respectively, in a Quantum Design cryostat (5–300 K). For the higher temperatures (300–900 K), ρ and *S* were measured using an Ulvac-ZEM3 apparatus.

III. RESULTS

A. RT structure

The RT x-ray diffraction (XRD) pattern is characteristic of the hollandite-type structure, as shown in Fig. 1; nevertheless, a small amount of $Pb_3V_2O_8$ is observed as impurity (~2% in weight). Due to its V^{5+} state ($3d^0$), $Pb_3V_2O_8$ is insulating and has been investigated for its ferroelectric properties.[14] Consequently, the presence of this insulating impurity cannot explain the transport properties. The structure is refined in the $I12/m1$ space group with $a=10.125$ Å, $b=2.902$ Å, $c=9.880$ Å, and $\beta=90.928°$. These values are close to those reported for hollandites such as $Ba_{1.2}Mn_8O_{16}$ (10.052 Å, 2.858 Å, 9.763Å; $\beta=89.96°$),[15] $Ba_2Mn_8O_{16}$ (10.006 Å, 2.866 Å, 9.746 Å; $\beta=91.17°$),[16] or $Pb_{1.32}V_{8.35}O_{16.7}$ ($a=9.887$ Å, $b=2.903$ Å, $c=10.108$ Å, and $\beta=90.84$ Å).[11] The difference with the latter could result from the difference in the Pb^{2+} content (and thus the average V oxidation state). The refinements lead to a V/Pb ratio close to 5.0 smaller than the 6.3 calculated for $Pb_{1.32}V_{8.35}O_{16.7}$.[11] This value however has to be taken with care because the quality of our data does not allow a deep structural study as the one in Ref. 11 for a single crystal.

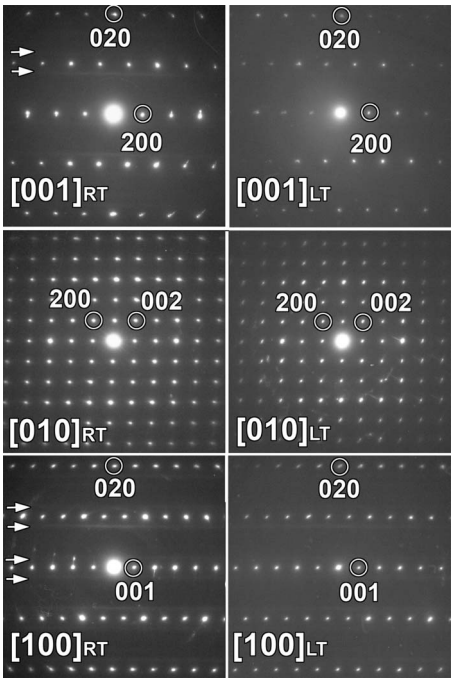

FIG. 2. Electron-diffraction patterns along the main zone axes for $Pb_{1.6}V_8O_{16}$ at room temperature (RT—left column) and low temperature (LT—right column).

In order to obtain more structural data, the room-temperature ED patterns of $Pb_{1.6}V_8O_{16}$, taken along the major zone axes, are shown in the left panels of Fig. 2. They can be completely indexed in the $I12/m1$ space group using the unit-cell parameters obtained by x-ray powder diffraction. The energy dispersive spectroscopy (EDS) analysis results averaged over several microcrystals crystallizing in the hollandite structure yield a V/Pb ratio equal to 5.0, consistent with the value extracted from the structural refinements. A high-resolution transmission electron microscopy (HRTEM) study has been performed along the most relevant [010] direction where the structure can be interpreted in the terms of cation and oxygen columns (Fig. 3). Image simulations, based on the $I12/m1$ structural parameters obtained from XRD, indicate that the dark dots on this image (see enlargement in Fig. 3) correspond to heavy cation columns. In particular, the central darker spots correspond to Pb columns whereas the eight less dark surrounding dots locate the V atoms. A detailed analysis of different areas and crystals only revealed a perfectly crystalline structure, free of any defects or structural modulations.

B. Electronic-transport and magnetic properties

Hollandites vanadates $Bi_xV_8O_{16}$ and $K_2V_8O_{16}$ are known to exhibit a metal-insulator transition MIT.[9,10] The $\rho(T)$

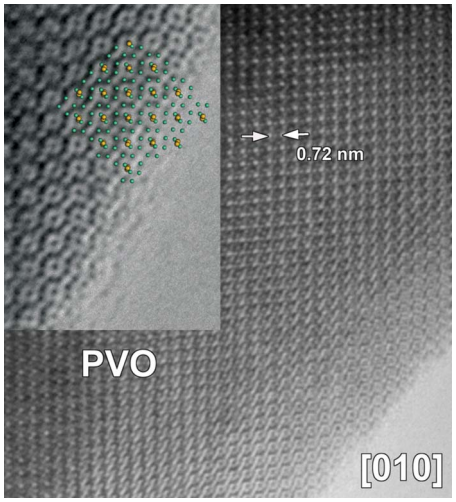

FIG. 3. (Color online) HRTEM image of $Pb_{1.6}V_8O_{16}$ along the [010] zone axis. An enlargement image and overlay structural model are given as an inset where Pb and V are yellow and green correspondingly. According to the calculated images, the dark dots represent heavy atoms columns.

curve collected from 5 to 900 K for the present PbVO vanadate [Fig. 4(a)] reveals also a strong localization starting below about ~200 K with a clear kink at 140 K. Above 200 K, ρ remains well below 10^{-2} Ω cm, reaching almost constant values of ~2 mΩ cm for $300<T<900$ K, following a small polaron model [$\rho/T\sim\exp(E/T)$] [Fig. 4(b)]. This value is very constant, ranging here in this large T interval between 1.7 and 2.2 mΩ cm. This conduction regime at high T is in marked contrast with the strong localization observed below ~200 K with a kink at 140 K, ρ reaching a value of 10^6 Ω cm at 20 K. This low-T localized behavior can be fitted by a three-dimensional (3D) variable-range hopping model [Fig. 4(c)]. In the previous reports, the existence of V^{3+} and V^{4+} charge orbital ordering (COO) phenomena have been invoked to explain the MIT of hollandite vanadates with commensurate V^{3+}/V^{4+} ratios.[9,10] According to the structural study leading to the approximate $Pb_{1.6}V_8O_{16}$ formula, the V oxidation state is formally $\nu_V=3.6$. As this value, intermediate between those in $K_2V_8O_{16}$, ($\nu_V=3.75$) and $Bi_{1.8}V_8O_{16}$ ($\nu_V=3.32$), is not near a commensurate value, similar COO might not be active in $Pb_{1.6}V_8O_{16}$. However, the T dependence of the magnetic-susceptibility $\chi(T)$ curve shows a χ reduction in the vicinity of the resistivity transition temperature with a χ_{min} at 140 K (Fig. 5). According to Ref. 17, such a χ reduction might reflect COO setting with the creation along b of antiferromagnetic (AFM) V^{4+}-V^{4+} and V^{3+}-V^{4+} chains in the double rutile stripes of the $(VO_6)_2$ infinite ribbons. The transition temperature is close to the one observed in V_2O_3 with $T_N=168$ K.[18] Also AFM transitions are observed in $La_{1-x}Sr_xVO_3$, between 150 and 100 K, and again for a V oxidation state close to 3 ($x<0.2$).[19] Here, in this hollandite structure, a similar transition can be observed for a larger doping $\nu_V=3.6$. However, the comparison of the field-cooled cooling (fcc) and field-cooled warming (fcw) curves (inset of Fig. 5) does not allow to reveal an hysteresis at the magnetic transition: this is also supported by the reversibility of the $\rho(T)$ curves, collected

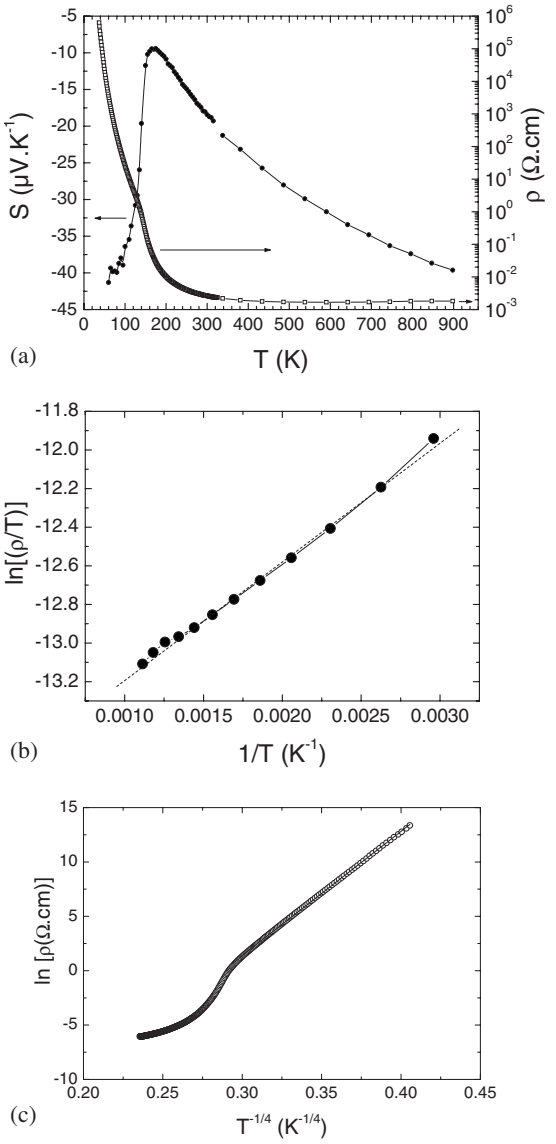

FIG. 4. (a) T dependence of the Seebeck coefficient S (left y axis) and the electrical resistivity (ρ) (right y axis). (b) High-T fit of $\ln(\rho/T)$ as a function of $1/T$, following a small polaron model. (c) $\ln\rho$ as a function of $T^{-1/4}$ showing the 3D VRH behavior observed at low T.

upon decreasing or increasing T, in the T_{MI} region. These results suggest a lack of a first-order transition related to the COO which contrasts with the reports for $K_2V_8O_{16}$,[10] the χ anomaly corresponding to an antiferromagnetic transition.

The lack of COO and associated structural transition has been checked by TEM and x-ray diffraction collected at RT and 100 K. The ED patterns taken at 100 K (Fig. 2 right) do not show any extra reflections compared to those taken at RT (Fig. 2 left) and therefore no evidence for the formation of a superlattice or of a lowering of the symmetry. This points toward a lack of structural transition at T_{MI}. In addition, the angles and distances between the diffraction spots have slightly changed. This is confirmed by the only small contraction of the unit-cell volume varying by only 3.3% from 300 to 100 K. This is also supported by the only slight decrease (<0.1°) in the β monoclinic angle measured on the

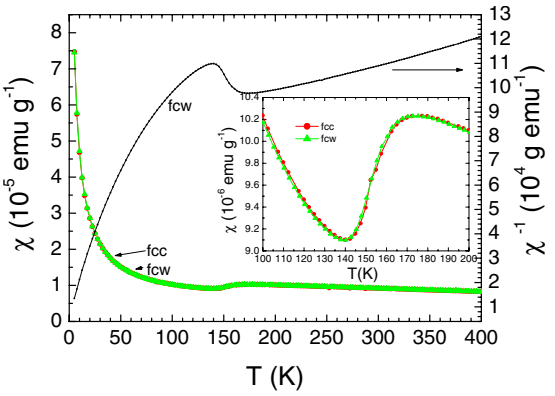

FIG. 5. (Color online) T-dependent magnetic susceptibility ($\chi=M/H$) collected in 0.3 T. Inset: fcc and fcw $\chi(T)$ curves in the T_{MI} region.

ED patterns and also confirmed by the values refined from x-ray diffraction data, from 90.928(5)° at RT to 90.871(5)° at 100 K. Thus, these structural characterizations allow to rule out a COO phenomenon or a structural transition at T_{MI}. At maximum, the coupled magnetic and transport transitions at T_{MI} involve a slight structural distortion. This would deserve a further neutron-diffraction study.

The metal-insulator transition at ~140 K can also be easily detected by Seebeck measurements [Fig. 4(a)]. The corresponding $S(T)$ curve indicates that for all T for which S is measurable (50–900 K), the S value is negative and moreover that a clear transition exists with a midpoint near 140 K, i.e., in good agreement with the transition detected by both ρ and χ measurements. This transition is rather abrupt: S varies by 20 μV K^{-1} as T decreases by only 20 K (from 150 to 130 K) whereas in the metallic regime, S varies only by ~3 μV K^{-1} as T increases by 100 K (from 150 to 250 K). The sharpness of the transition at T_{MI} on the $S(T)$ curve is consistent with the existence of a magnetostrictive effect at T_{MI} as the long-range antiferromagnetism sets with $|S|$ increasing as T decreasing below T_{MI} due to charge localization.

The resistivity can be described by a small polaron model at high T but the high-T part of S does not follow this small polaron description. It rather follows a T^{α} behavior, with $\alpha \sim 0.33$, which could be associated to 2D VRH (Fig. 6).

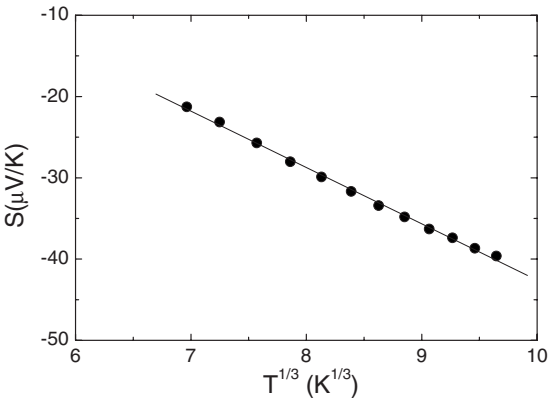

FIG. 6. High-T Seebeck coefficient S as a function of $T^{1/3}$.

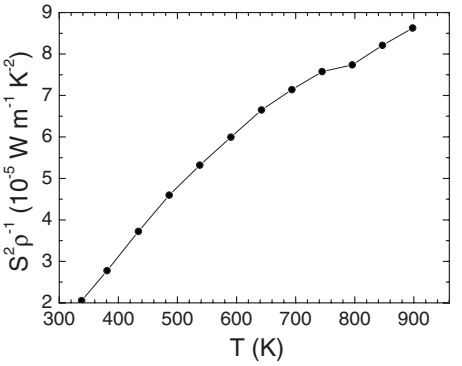

FIG. 7. T dependence of the power factor (PF=S^2/ρ).

Understanding this inconsistency and its relationship with the complex crystallographic structure is very important as these T dependences are of interest for the TE power factor: the value of power factor (PF) increases with T reaching a maximum of 8.5×10^{-5} (Fig. 7) at 900 K.

To explain the negative sign of S at high T ($T \gg T_{MI}$), one has to consider the empty degenerated t_{2g} orbitals of V^{5+} (d^0). Adding electrons in this starting state up to $V^{3.6+}$ consists in the filling of the t_{2g} orbitals below half filling and it implies a transport dominated by electrons. According to Marsh and Parris,[5] the spin and orbital degeneracy terms in the absence of a magnetic coupling (which is indeed the case for $T \gg T_{MI}$), for a V^{3+} (d^2)/V^{4+} (d^1) mixture lead to a $S_{T\to\infty}$ value of ~−35 μV K^{-1}. Although the $S(T)$ curve in Fig. 4(a) does not show a clear tendency toward saturation even at 900 K, the experimental $S_{900\ K}$ value of ~−38 μV K^{-1} is near the calculated expectation. The spin entropy term seems to dominate the Seebeck coefficient. The lack of a metallic S vs T dependence in $Pb_{1.6}V_8O_{16}$ beyond T_{MI} could be related to the different pathways for the charge carriers transfer in the structure. In the rutile ribbon itself, charges can be exchanged between the V cations nearest neighbors via the bridging oxygen anions but the corresponding V-O-V angles of ~90° are probably not very favorable. In contrast, the short V-V distance (along the b axis, i.e., the direction of the ladder), could facilitate a direct exchange between the t_{2g} orbitals. Additionally, the connections between the double ribbons open pathways in the perpendicular direction through shared oxygen anions between non equivalent V cations. This complexity related to the transport anisotropy was evidenced in crystals of rhodate and ruthenate hollandites.[17,20] It showed that the $\rho_{(a,b)}/\rho_{(c)}$ ratio increases as T decreases reaching for instance at 4.2 K a factor of 13 for tetragonal $K_2Ru_8O_{16}$.[20] This indicates that the transport becomes more 1D as T decreases, i.e., the hopping between corner-sharing adjacent double ribbons decreases. In contrast, at much higher T, the charge transport perpendicular to the ladders cannot be neglected anymore, leading to a more 3D transport behavior. In the case of $Pb_{1.6}V_8O_{16}$, the transport is completely different as a strong localized behavior is observed below T_{MI}, with a 3D variable-range hopping regime fitting the $\rho(T)$ curve, in good agreement with a localization induced by the antiferromagnetic coupling between V cations. In this localized situation, transport seems to be more 3D than for the metallic hollandites, due to this long-range magnetic ordering.

IV. CONCLUSION

The present study of the transport properties up to $T=900$ K demonstrates that hollandite vanadates can be viewed as *n*-type bad metals. Although measurements on textured material are required for the determination of the anisotropic properties, the $|S|$ values reached at 900 K are still too low for applications. Furthermore, tailoring the oxidation state of the vanadium, in between V^{3+} and V^{4+}, would not allow changing significantly the Seebeck values. In the present case, d^1/d^2 spin and orbital degeneracies (and not the band filling) govern the absolute S values at high T.

ACKNOWLEDGMENT

This work was supported by the FP7 European Initial Training Network SOPRANO (Grant No. GA-2008-214040).

*FAX: 02.31.95.16.00; antoine.maignan@ensicaen.fr

[1] Y. Tokura and N. Nagosa, Science **288**, 462 (2000).
[2] F. D. M. Haldane, Phys. Rev. Lett. **50**, 1153 (1983).
[3] *Thermoelectric Oxides*, edited by K. Koumoto (Research Signpost, India, 2002).
[4] W. Koshibae and S. Maekawa, Phys. Rev. Lett. **87**, 236603 (2001).
[5] D. B. Marsh and P. E. Parris, Phys. Rev. B **54**, 7720 (1996).
[6] A. Maignan, C. Martin, F. Damay, B. Raveau, and J. Hejtmanek, Phys. Rev. B **58**, 2758 (1998).
[7] A. Byström and A. M. Byström, Acta Crystallogr. **3**, 146 (1950).
[8] A. Niazi, S. L. Bud'ko, D. L. Schlagel, J. Q. Yan, T. A. Lograsso, A. Kreyssig, S. Das, S. Nandi, A. I. Goldman, A. Honecker, R. W. McCallum, M. Reehuis, O. Pieper, B. Lake, and D. C. Johnston, Phys. Rev. B **79**, 104432 (2009).
[9] H. Kato, T. Waki, M. Kato, K. Yoshimura, and K. Kosuge, J. Phys. Soc. Jpn. **70**, 325 (2001).
[10] M. Isobe, S. Koishi, N. Kouno, J.-I. Yamaura, T. Yamauchi, H. Ueda, H. Gotou, T. Yagi, and Y. Ueda, J. Phys. Soc. Jpn. **75**, 073801 (2006).
[11] O. Mentre and F. Abraham, J. Solid State Chem. **125**, 91 (1996).
[12] M. Imada, A. Fujimori, and Y. Tokura, Rev. Mod. Phys. **70**, 1039 (1998).
[13] J. Rodríguez-Carvajal, Physica B **192**, 55 (1993).
[14] P. Garnier, G. Calvarin, J.-F. Berar, and D. Weigl, Mater. Res. Bull. **19**, 407 (1984).
[15] S. Ishiwata, J. W. G. Bos, Q. Huang, and R. J. Cava, J. Phys.: Condens. Matter **18**, 3745 (2006).
[16] H. Miura, Mineral. J. **13**, 119 (1986).
[17] S. Horiuchi, T. Shirakawa, and Y. Ohta, Phys. Rev. B **77**, 155120 (2008).
[18] W. Bao, C. Broholm, S. A. Carter, T. F. Rosenbaum, G. Aeppli, S. F. Trevino, P. Metcalf, J. M. Honig, and J. Spalek, Phys. Rev. Lett. **71**, 766 (1993).
[19] P. Dougier and P. Hagenmuller, J. Solid State Chem. **15**, 158 (1975).
[20] W. Kobayashi, Phys. Rev. B **79**, 155116 (2009).